# SMART:
# Modular Architecture for Reliable Transportation

Savvas Papadopoulos[1], Alessandro Galassini[2], Laimonas Ruksnaitis[4], Nabilah Farhat[3], Oleh Kiselychnyk[4], Will Midgley[3], Michele Degano[2]

| | | | |
|---|---|---|---|
| [1]*School of Engineering and Built Environment* *Edinburgh Napier University* Edinburgh, UK s.papadopoulos@napier.ac.uk | [2]*Power Electronics, Machines and Control Group* *University of Nottingham* Nottingham, UK alessandro.galassini@nottingham.ac.uk michele.degano@nottingham.ac.uk | [3]*Control Systems Group* *Loughborough University* Loughborough, UK n.farhat@lboro.ac.uk w.midgley@lboro.ac.uk | [4]*Power and Control Systems Research Laboratory* *University of Warwick* Coventry, UK L.Ruksnaitis@warwick.ac.uk O.Kiselychnyk@warwick.ac.uk |

*Abstract*—This paper proposes a new ultra-reliable architecture for fully electric propulsion primarily aimed at the automotive sector. The system considers a direct drive arrangement, minimizing the number of moving components and is based on a network of multi-three-phase machines providing propulsion. The DC-link from each 3-phase star within each machine can be interconnected to form a network, or mesh, which would allow a variety of post-fault mitigation strategies. The system scaling is considered along with the benefits and impact of modularity on device ratings. Finally the simulated performance for one drive is presented demonstrating the core capability in redirecting power flow in case of a fault.

*Keywords—reliability, multi three phase, automotive transportation, electric propulsion, fault strategy*

## I. INTRODUCTION

The electrification of transportation is at the forefront of both industrial and academic development at a time when international governments have set ambitious targets for the reduction of greenhouse gases. The transport industry is attributed as one of the major contributors of carbon emissions and as such, the UK government will ban all new petrol and diesel cars as of 2040 [1]. Similar plans are afoot in France and the rest of Europe, as a commitment to clean air policy. Fully electric propulsion will be widely adopted within the next few decades, eventually making traditional combustion engines obsolete.

While important strides have been taken in improving electric vehicle technology, the disjointed nature of the automotive sector and the early stage of adoption mean that there is a lack of industry standardisation of voltage levels, system architectures and alignment of development goals.

With the emergence of technologies such as autonomous fully electric vehicles, safety and reliability is expected to become a major theme. In addition, current methods for powering pure electric vehicles suffer from a lack of reliability – a single point of failure can bring the whole vehicle to a standstill, compromising the safety of the passengers and other road users.

The aim of this paper is to propose a system architecture combining both reliability and fault tolerance in order to deliver a system focused on safety. The system also takes advantage of modularity and flexibility in the aspects of power electronics, control and machine design.

The first section of this paper will cover the literature around multi-three-phase motor research and their control which is the enabling technology for this system. The second section will introduce electric vehicle drivetrains establishing what is considered the conventional arrangement, and it will then introduce the proposed arrangement. The third section investigates how the system scaling is affected by modularity. Its impact on different aspects is quantified either analytically or via simulations. Finally the simulated performance is presented. The basic building block of the system is identified and its functionality is shown under different conditions including simulations within the full system

### A. Multi-three phase machines

Multi-three-phase machines are a newly-developed enabling technology that allows for a flexible response to changing demand within the electrical machine. The machine windings are typically split into numerous sets of 3-phase systems physically displaced by a fixed angle. Typically these machines have a higher complexity in modelling and control as the interaction and cross coupling between phases must be considered, leading to a complicated inductance matrix [2-7].

Recent technological advancement in power flow control has shown that the load sharing can be controlled between the numbers of systems [2, 4-5]. Control can be either centralised or even decentralised [3] for higher reliability. Solutions typically use vector space decomposition for control in the synchronous reference frame [2-3, 5]. Efforts have already been made to integrate multi-three-phase machines for direct-drive and integrated in-wheel applications [8-9] where it has been shown that high torque density can be achieved [10-11]. The proposed system considers multi-three-phase machines as the enabling technology. The increase in computational power of modern digital controllers and the emergence of more efficient power semiconductors enhances the capability of this technology to achieve high efficiency and reliability compared to traditional powertrain solutions as will be outlined in the next sections.

## II. ELECTRIC VEHICLE DRIVETRAINS

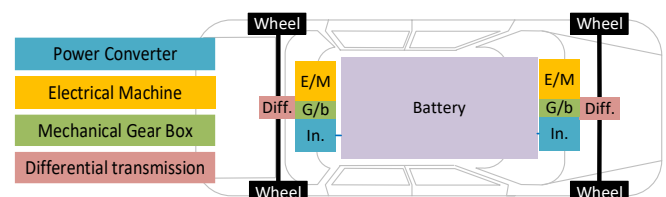### A. Conventional electric vehicle drivetrain



Fig. 1: Conventional layout of an Electric Vehicle drivetrain

The layout of conventional drivetrain of an electric vehicle is shown in Fig. 1. A gearbox is used to increase the mechanical output torque transferred to the wheels via a differential transmission. High power density is an important factor in transportation and to achieve it in this configuration, high speed machines are opted for, since the increase of the fundamental frequency is associated with a decrease in size. Typical maximum speeds approach 20000 rpm where a gearbox ratio of around 9:1 is used to reduce the speed of the wheel to around 2200 rpm, depending on the radius of the intended wheels and the maximum speed. All-Wheel-Drive (AWD) capability, typically found in high end models, is implemented by using separate machines to drive the front and back wheels. These could be scaled equally giving a 50:50 torque capability between the front and back wheels or following an asymmetric arrangement, where a main motor is rated close to the maximum power whilst the second motor behaves as an auxiliary one to provide better traction and additional power. High end commercial vehicles are rated between 300 kW to 400 kW with around 1000 Nm of torque.

In the case of an electrical fault occurring in the motor, a two-wheel drive (2WD) system could be fully compromised whilst an AWD will benefit from the redundancy and could continue operating, albeit at a significantly reduced power level. When further faults are considered, the vulnerability of the system is revealed. A fault in the battery bank could bring the system to standstill if the fault is not isolated. Mechanical failures are also likely to occur due to the numerous components within the gearbox and transmission.

There are a few notable and well publicized failures of electric vehicles where the severity of the fault has been exacerbated by the flammable and toxic nature of lithium-based batteries [12]. This emphasizes the importance of fault-tolerance which must be designed into the system. The use of high current-rated converters (up to 1.5 kA) in current systems makes it more challenging to isolate a fault, particularly if a paralleled switch arrangement is opted for. Finally, more moving parts make mechanical damage more likely.

### B. SMART vehicle drivetrain

The proposed drivetrain is designed bearing in mind reliability and fault tolerance from the onset. Rather than using a single machine and drive for propulsion, the proposed system envisions a mesh of identical nodes interconnected with multi-three-phase machines and multiple DC sources.

A simplified configuration is depicted in Fig. 2 considering only two wheels. Each wheel is mechanically driven directly (no gearbox) by a 9-phase electrical machine, which can be considered as 3 separate 3-phase systems. Each of the three stars contributes equally to the mechanical torque thus the rating of the converters is scaled by the number of systems, three in this case. The dc-link of each converter from the same machine is connected to a separate dc source. By interconnecting the dc sources from the two machines, three separate power paths are created. The segmentation is therefore carried on from the machine to the drives as well as the batteries.

Each machine can be defined as a power node and a "roundabout" of energy exchange, meaning that power can be exchanged among different stars. Thus when a failure occurs at any point, energy can be rerouted and still flow to functional nodes. The interconnected mesh allows for redundancy to be designed into the system from the start, ensuring that a single
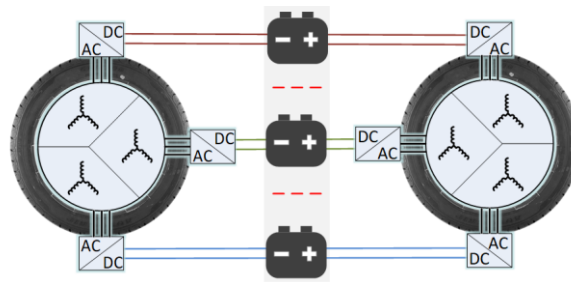


Fig. 2: Simplified diagram illustrating the connections between two 9-phase in-wheel machines.

component failure will not cause a whole system failure – guaranteeing system reliability.

Each node is locally self-controlled and can support neighbouring nodes in case of faults. A high level of reliability is achieved by combining the redundancy of the modular converters and multiple stator windings of the motors. When considering a full vehicle of four machines, multiple options are possible as shown in Fig. 3. Each option considers different paths and interconnections as well as different segmentation of the batteries, shared by two or more inverters. The decision about which system is optimal will depend on a given design and should be investigated among the multitude of possible options.

The following are the overall benefits of the proposed system:

- Embedded redundancy

- Better vehicle weight distribution

- Modularity/Scalability/Configurability

- Possibility of torque vectoring

- Scope for multi-variable optimisation between cost, weight, efficiency, thermal performance etc.

- Optimisation for loss management around the mesh, advanced control of the power flows through the mesh and refining/redesigning the basic nodes and their performance
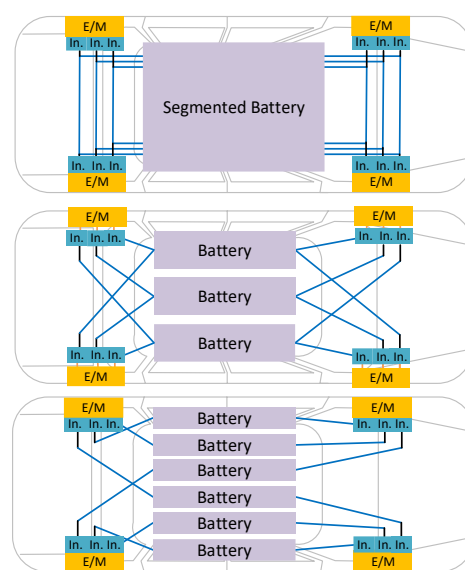


Fig. 3: Examples of system connections based on an AWD vehicle using 9-phase machines considering different battery segmentation

## III. SYSTEM SCALING

This section presents the results of the analytical investigation towards the system scaling and the impact of segmentation considering a high-end passenger vehicle. TABLE 1 shows the system requirements for the overall vehicle which reflect the current top range vehicle specs.

*TABLE 1. System Scaling Parameters*

| Parameter | Min | Max |
|---|---|---|
| System torque | - | 3200Nm |
| Maximum wheel speed | - | 2300rpm |
| Vehicle peak power | 200kW | 800kW |
| DC bus Voltage | 400V | 800V |

From a mechanical perspective, AWD is assumed therefore the total vehicle torque is divided by the number of wheels, four in this case, where each can provide 800Nm. The motor mechanical speed is given by the maximum vehicle velocity and the wheel diameter. Considering 18 inch (46cm) wheels and 200 km/h this is set at 240 rad/s.

Segmentation and subsequently modularity is a central theme to the proposed concept. In order to assess expected benefits and implementation feasibility, and to quantify the limitations of a possible solution, multiple aspects must be considered which may be interlinked.

The impact of machine segmentation on the current ratings is straightforward. For a given machine constant the current needed to deliver the full torque is divided by the number of three phase systems $N$.

The machine constant is proportional to the number of poles and the machine flux. Increasing the number of pole pairs will increase the output torque. However, this will also increase the fundamental electrical frequency which relates the mechanical speed to the number of poles. Considering the inverter switching frequency must be at least 20 times higher than the fundamental frequency. This means that the number of poles will be restricted by the switching frequency as well as by physical space constraints.

The problem is visualised in Fig. 4 and Fig. 5 where the number of pole pairs and the switching frequency are shown against the nominal current and the number of three phase systems in the machine. An overall trend can be observed showing that as the number of systems increases the number of pole pairs decreases for higher nominal currents. If the nominal current is decreased too much then the number of poles required becomes unfeasible as well as the switching frequency. Furthermore, the graphs show that a wide range of solutions is possible for a given total torque for which more assessment may be necessary to identify optimal solutions.

In order to assess the impact of higher switching frequency at different nominal currents for power electronics a simulation has been used.

The thermal models for different switching devices have been included into PLECS. Devices rated at various current levels have been considered along with different technologies and packaging solutions, ranging from discrete devices to power modules and silicon based IGBT/Mosfet to Silicon Carbide (SiC) devices from a range of leading manufacturers
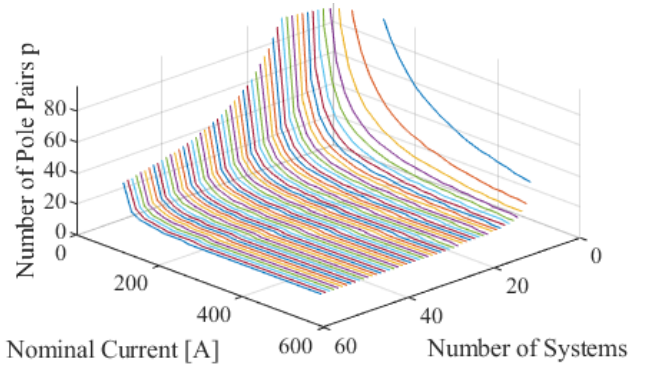


Fig. 4: Number of pole pairs relationship over different nominal current values for a different number of systems
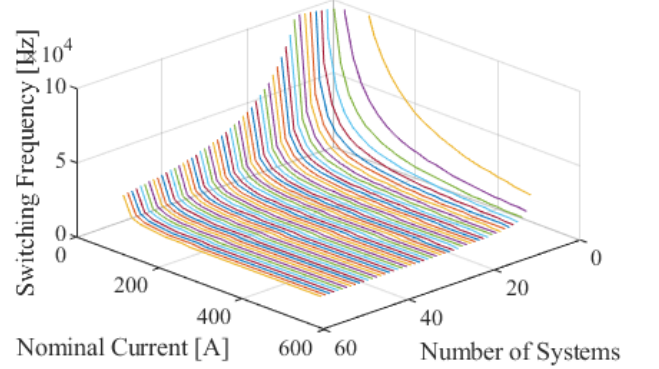


Fig. 5: Switching frequency variation over different nominal current values for a different number of systems
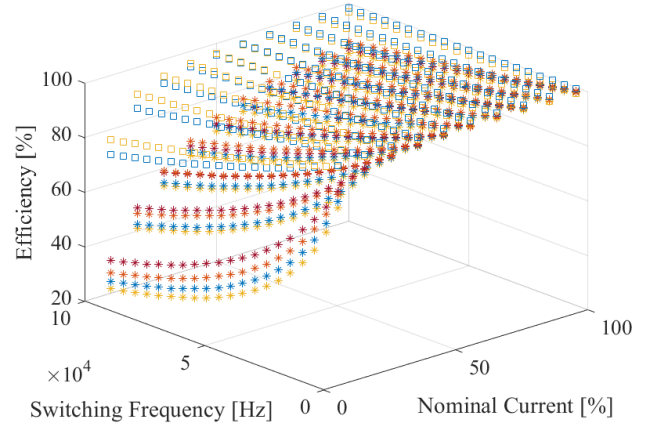


Fig. 6: Cumulated simulation results for power semiconductor efficiency over the nominal current range considering different switching frequencies

Manufacturer provided models have been used where available whilst, if unavailable, bespoke models have been created based on available datasheet information.

An automated simulation has been run to evaluate the semiconductor losses at different load levels and switching frequencies for each device. A 3-phase two-level Voltage Source Inverter (VSI) topology has been used with the load adjusted at different percentages compared to the device nominal current. The efficiency accounts for the full converter. Two voltage categories have been considered with the devices compared separately for a 400V or 800V DC level. Selected cumulated results can be seen in Fig. 6 where the efficiency of the full converter is shown against the switching frequency and nominal current. Each colour represents a different device (SiC in squares, Si in asterisks).
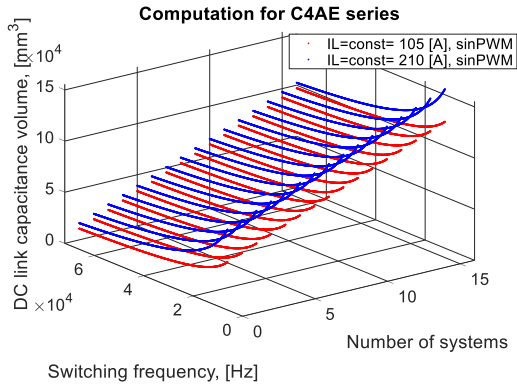
*Fig. 7: Required DC link capacitance volume as a function of N and switching frequency*

The following conclusions can be reached. Devices rated with higher currents show a higher drop of efficiency with increasing switching frequency and significantly poorer efficiency at low modulation indexes (low loads). SiC devices (squares) offer significantly superior performance, especially at higher switching frequencies compared to Si devices (asterisks). The above supports the hypothesis that segmentation enables the use of a bigger number of lower rated devices to benefit the overall efficiency of the drivetrain, and particularly at low loads.

Analytical computations have been carried out in order to find the variation of the DC-link capacitance size considering different levels of segmentation, accordingly to the methodology from [13] for sinusoidal PWM. The results are depicted in Fig. 7 for commercially available C4AE capacitor series and two total load currents assuming 5% of the DC-link voltage ripple, unity load power factor and unity amplitude modulation index. It can be observed that the capacitance volume increases for a higher number of systems, mainly attributed to the fact that higher packaging and insulation is needed for this scenario i.e. $N$ capacitors providing the required capacitance are bigger than one big capacitor of the same value. However as the switching frequency increases, the DC-link capacitance can be minimised for a permitted level of DC voltage ripple.

A preliminary estimation has been carried out in order to capture the trend of the variation of volume and mass of the powertrain for different levels of segmentation.
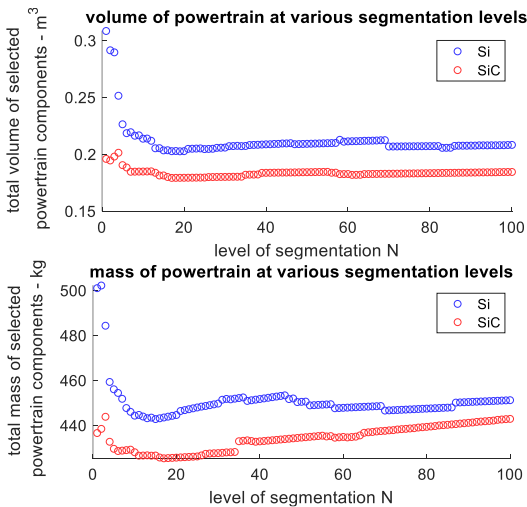




*Fig. 8: Estimated mass and volume of the drivetrain over different levels of segmentation for Silicon (Si) and Silicon Carbide (SiC) devices*

The plots, shown in Fig. 8 account for switching devices, batteries, inverter cooling system and DC-link capacitors. The computations are based on datasheets of commercially available devices and components. 26 Si IGBT and SiC MOSFET devices were characterised in PLECS software. Then 23,929 powertrain configurations were generated of equivalent power and capacity. Proportional approximations were used for component masses and costs estimations. Optimal mass and volume configurations were found for each $N$ and device technology combination and plotted as a function of $N$. The overall results suggest a balance can be reached between the performance, size, weight and presumably the cost of the drivetrain solution.

## IV. PERFORMANCE EVALUATION

In order to validate the feasibility of the proposed idea two sets of simulations are presented. Both simulations consider a system based on a 9-phase motor scaled according to the full test vehicle specifications.

### A. Power Electronics simulation results

A PLECS simulation has been built in order to validate the basic functionality of a multi-three-phase machine as a multifunctional node, as required in the proposed application. TABLE 2 shows the simulated parameters of a multi-three-phase electric motor coupled to a prime mover spinning the shaft of the machine under test at 240 rad/s, the maximum speed which would bring the vehicle at 198 km/h. The implemented algorithm is the Field Oriented Control for three-phase Surface Permanent Magnet machines. No flux weakening has been considered. In order to control the nine phase currents, six Proportional-Integral controllers – three along the d axes and three along the q axes – have been designed accounting for the values of the first harmonic inductances. In the simulation, three isolated 2-Level Voltage Source Inverters (2LVSI) have been connected to three isolated 800V Battery Packs (BPs) based on a non-linear battery model [14].

*TABLE 2. Simulated Parameters per single inverter*

| Parameter | Symbol | Value | Unit |
|---|---|---|---|
| Fundamental electrical freq. | $f_e$ | 1.22 | kHz |
| Switching frequency | $f_{sw}$ | 36.76 | kHz |
| First harmonic inductances | $L_{d1}, L_{q1}$ | 128.3 | uH |
| Phase resistance | $r_s$ | 11.3 | $m\Omega$ |
| DC-link Capacitor | $C_{DC}$ | 92 | uF |
| Current filter bandwidth | $\omega_{fc}$ | 100 | kHz |

Three operating conditions have been considered and presented in the following paragraphs. Figure 9 shows the AC currents in steady state motoring operation. The three transformed respective $i_q$ currents within each star, shown in Fig. 10, are producing an overall wheel torque of 806 Nm (Fig. 11) with three DC-links showing the battery voltages at 802 V (Fig.12). The motor performance achieved is in line with the designed operating point thus validating the model and confirming the functionality of the control scheme.
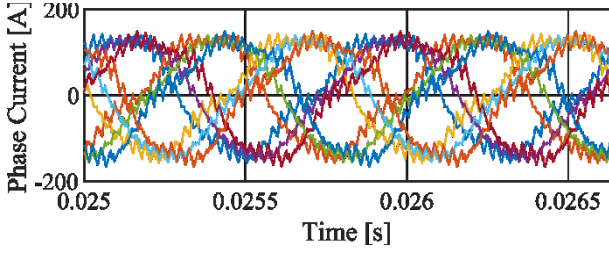
- **Steady-state motoring operation:**



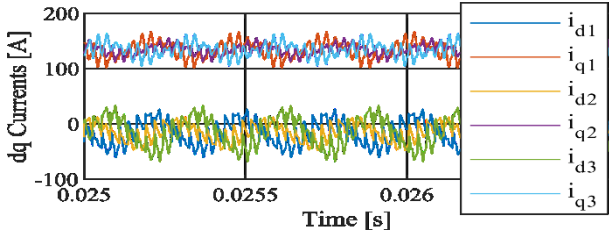Fig. 9: Nine phase currents at nominal speed



Fig. 10: dq transformed currents at nominal speed.
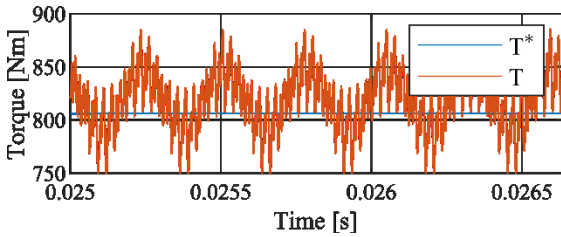


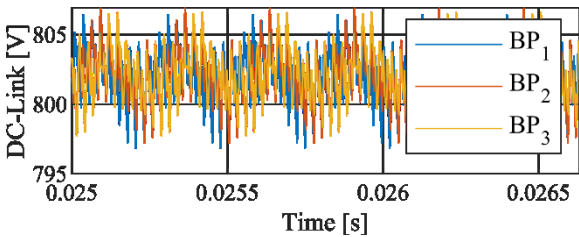Fig. 11: Reference and measured total torque



Fig. 12: Three Battery Pack (BP) voltages

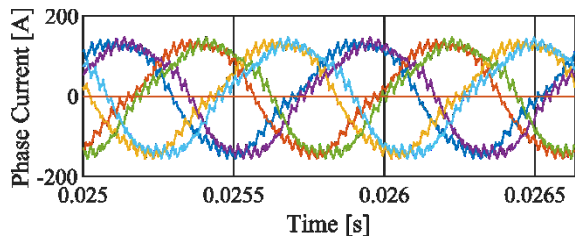- **Steady-state operation with one star in open-circuit:**



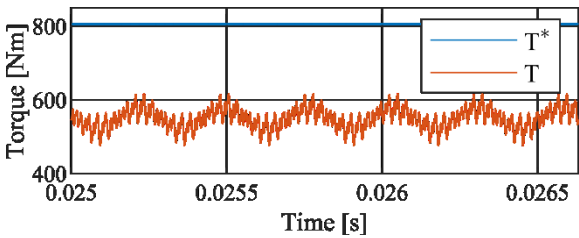Fig. 13: Terminals of the last set of windings are not connected.



Fig. 14: Available torque in case of open circuit fault.

In case of open circuit fault in one of the inverters, only six currents out of nine are regulated (Fig.13) and two thirds of the nominal torque are delivered to the shaft (Fig. 14). As

in a real case scenario where fuses would be installed along the lines, the short circuit fault has not been considered. In case of short circuit, the phase currents would rapidly increase while blowing the fuses and isolating the faulty segment of the system [10].

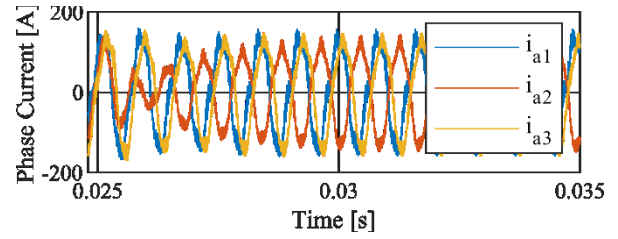- **Transient operation showing regeneration mode:**



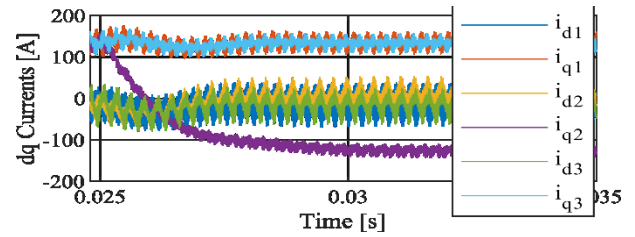Fig. 15: Phase a currents during regeneration mode



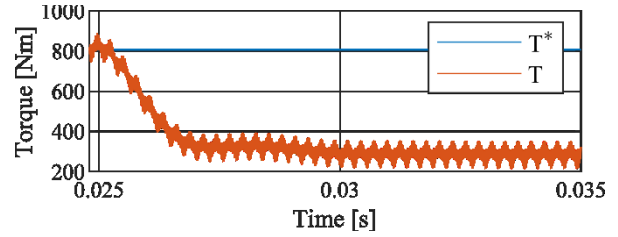Fig. 16: dq transformed currents during regeneration mode.



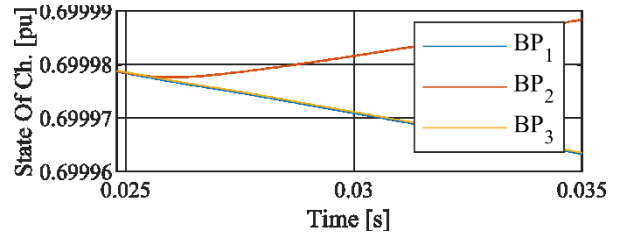Fig. 17: Available torque during regeneration mode.



Fig. 18: State Of Charge of the battery packs during regeneration mode

A simulation has been completed to show the transient operation considering one star in regeneration mode, where one of the battery packs is charged from the adjacent stars. The current transients are shown in Fig. 15 and Fig. 16 along with the impact on the torque, which is reduced to one third (Fig. 17). The operation is validated in Fig. 18 showing the BP State of Charge (SOC) reflecting the expected change in power flow. The result thus concludes the validation of the basic functionality of a multi-three phase machine as a multifunctional node.

### B. Full system simulation results

A second simulation has been set up considering an AWD system based on 9-phase machines and the vehicle mechanical model the results of which are presented here focusing on the longitudinal behaviour. The model considers the aerodynamic drag and the rolling resistance of the vehicle.
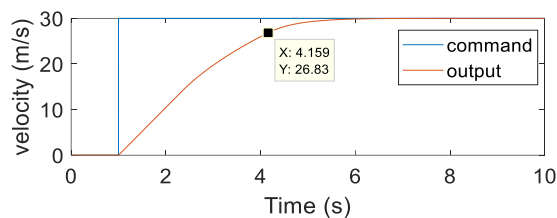
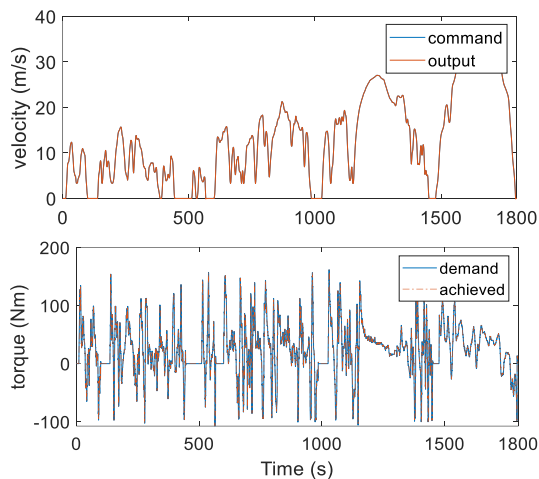*Fig. 19: Step response to a vehicle velocity demand from standstill*



*Fig. 20: WLTP drive cycle showing torque and velocity demand along with the achieved performance*

Fig. 19 shows the vehicle response to a step velocity demand. The vehicle can accelerate from 0-60mph (28.83m/s) in 4.16s, on par with high end electric vehicle models and in line with the design goals.

To achieve a preliminary indication of the full vehicle performance the model has been run over the Worldwide Harmonised Light Vehicle Test Procedure (WLTP) drive cycle over a period of 30minutes (1800s). The results are depicted in Fig. 20 showing the vehicle torque and velocity. It can be observed that the achieved profile follows the demand with negligible error thus validating the effectiveness of the design and suitability as an electric vehicle.

## V. CONCLUSION

This paper has proposed a new reliable architecture for automotive propulsion based on multi-three-phase motors. Each motor can be considered as a node connected to identical converters which are interconnected in a mesh to provide multiple and redundant power paths. The scaling and segmentation for such a system has been outlined along with design constraints for its implementation.

Simulation results have validated the fundamental operation and functionality of one node in normal operation and under fault. Finally a full vehicle simulation has been presented over a WLTP drive cycle showing the system performance matches the design goals.

This research concludes the preliminary investigation into the feasibility of this system and opens the scenario for more thorough and in-depth investigations into this architecture. The option of having numerous system layouts has been identified and thus advanced optimisation is needed at many levels in order to identify ideas aiming towards implementation. The system will guarantee that in the scenario of one or even multiple faults occurring, the vehicle can continue its operation ensuring the trustworthiness of a fully electric propulsion future.

## VI. REFERENCES

[1] A. Asthana and M. Taylor, "The Guardian," 25 July 2017. [Online].https://www.theguardian.com/politics/2017/jul/25/britain-to-ban-sale-of-all-diesel-and-petrol-cars-and-vans-from-2040.

[2] Zoric, I.; Jones, M. & Levi, E., "Arbitrary Power Sharing Among Three-Phase Winding Sets of Multiphase Machines", IEEE Transactions on Industrial Electronics, 2018, 65, 1128-1139

[3] Y. Hu, Z. Q. Zhu and M. Odavic, "Comparison of Two-Individual Current Control and Vector Space Decomposition Control for Dual Three-Phase PMSM," in IEEE Transactions on Industry Applications, vol. 53, no. 5, pp. 4483-4492, Sept.-Oct. 2017. doi: 10.1109/TIA.2017.2703682

[4] I. Zoric, M. Zabaleta, M. Jones and E. Levi, "Techniques for power sharing between winding sets of multiple three-phase machines," 2017 IEEE Workshop on Electrical Machines Design, Control and Diagnosis (WEMDCD), Nottingham, 2017, pp. 208-215. doi: 10.1109/WEMDCD.2017.7947748

[5] A. A. Abduallah, O. Dordevic and M. Jones, "Multidirectional power flow control among double winding six-phase induction machine winding sets," IECON 2017 - 43rd Annual Conference of the IEEE Industrial Electronics Society, Beijing, 2017, pp. 8001-8006. doi: 10.1109/IECON.2017.8217403

[6] A. Galassini, A. Costabeber and C. Gerada, "Speed control for multi-three phase synchronous electrical motors in fault condition," IEEE EUROCON 2017 -17th International Conference on Smart Technologies, Ohrid, 2017, pp. 698-703. doi: 10.1109/EUROCON.2017.8011200

[7] M. Mengoni et al., "Control of a fault-tolerant quadruple three-phase induction machine for More Electric Aircrafts," IECON 2016 - 42nd Annual Conference of the IEEE Industrial Electronics Society, Florence, 2016, pp. 5747-5753. doi: 10.1109/IECON.2016.7793968

[8] Watts, A., Vallance, A., Fraser, A., Whitehead, A. et al., "Integrating In-Wheel Motors into Vehicles - Real-World Experiences," SAE Int. J. Alt. Power. 1(1):289-307, 2012, https://doi.org/10.4271/2012-01-1037.

[9] Watts, A., Vallance, A., Whitehead, A., Hilton, C. et al., "The Technology and Economics of In-Wheel Motors," SAE Int. J. Passeng. Cars - Electron. Electr. Syst. 3(2):37-57, 2010, https://doi.org/10.4271/2010-01-2307.

[10] C. J. Ifedi, B. C. Mecrow, S. T. M. Brockway, G. S. Boast, G. J. Atkinson and D. Kostic-Perovic, "Fault-Tolerant In-Wheel Motor Topologies for High-Performance Electric Vehicles," in IEEE Transactions on Industry Applications, vol. 49, no. 3, pp. 1249-1257, May-June 2013. doi: 10.1109/TIA.2013.2252131

[11] C. J. Ifedi, B. C. Mecrow, J. D. Widmer, G. J. Atkinson, S. T. M. Brockway and D. Kostic-Perovic, "A high torque density, direct drive in-wheel motor for electric vehicles," 6th IET International Conference on Power Electronics, Machines and Drives (PEMD 2012), Bristol, 2012, pp. 1-6. doi: 10.1049/cp.2012.0254

[12] S. Russolillo "The wall street journal", 04 Oct 2013, "Musk Explains Why Tesla Model S Caught on Fire",[Online], https://blogs.wsj.com/moneybeat/2013/10/04/elon-musk-explains-how-model-s-caught-on-fire/

[13] P.A. Dahono, Y. Sato, T. Kataoka, "Analysis and minimization of ripple components of input current and voltage of PWM inverters," IEEE Trans Industry Applications, Vol. 32, no. 4, July/Aug., 1996, pp. 945-950.

[14] O. Tremblay, L. Dessaint and A. Dekkiche, "A Generic Battery Model for the Dynamic Simulation of Hybrid Electric Vehicles," 2007 IEEE Vehicle Power and Propulsion Conference, Arlington, TX, 2007, pp. 284-289. doi: 10.1109/VPPC.2007.4544139